JOURNAL OF MATERIALS SCIENCE 23 (1988) 3764–3770

Structural properties of plasma-sprayed zirconia-based electrolytes

M. SCAGLIOTTI, F. PARMIGIANI
Cise – Tecnologie Innovative SpA, via Reggio Emilia 39, 20090 Segrate, Milano, Italy
G. SAMOGGIA, G. LANZI
Dipartimento di Fisica A. Volta, Università di Pavia, via Bassi 6, 27100 Pavia, Italy
D. RICHON
Battelle Institute, Centre de Recherche de Genève, 7 route de Drize, 1227 Carouge, Genève, Switzerland

Zirconia-based electrolytes, stabilized either with yttrium oxide or calcium oxide, were prepared in 100 to 200 μm thick layers by plasma spraying and densified by high-temperature vacuum sintering. The structure and the microstructure were investigated by optical microscopy, scanning electron microscopy, X-ray diffraction and Raman spectroscopy. The results are compared with the data we obtained on the powders used for plasma spraying and on single crystals. In the zirconia–yttria system, dense and fully stabilized zirconia films with structural properties similar to the corresponding single crystals were obtained. On the other hand, cracks and deformations were observed on calcia-stabilized films. This phenomenon is explained by the dramatic increase of monoclinic phase content due to the preferential evaporation of calcium oxide which occurs during high-temperature vacuum sintering.

1. Introduction

Stabilized zirconia is widely used as electrolyte in high-temperature solid oxide fuel cells (HTSOFC), oxygen sensors and other electrochemical devices [1, 2]. In potentiometric oxygen monitors it can be used in the form of massive sintered material, while thin and thick films are indicated in HTSOFC and chemical reactor technology where minimum overall impedances and high active surface/volume ratios are required. Electrochemical vapour deposition [3], plasma spraying [4] and, more recently, tape casting [5] have been successfully employed in the fabrication of HTSOFC prototypes. However, only a limited number of works have been devoted to the correlation between chemical composition, structure, microstructure, electrical properties and preparation conditions of zirconia-based electrolyte films [6–8]. They deal with the properties of zirconia films prepared by physical vapour deposition [6, 7] or the doctor blade technique [8]. Plasma-sprayed zirconia films have been investigated only in view of applications as thermal barriers and protective coatings [9–11] and, as far as we know, no data have been published on their electrical properties.

It is worthwhile to point out that the high temperatures involved in the plasma-spraying process, the rapid quenching of the melted zirconia drops on the cold substrate during deposition, and the thermal treatments required to improve the film density, can affect the structure and modify the electrical properties of sprayed films with respect to sintered materials and single crystals. These considerations have stimulated the present investigation on plasma-sprayed zirconia electrolytes.

Plasma-sprayed films were prepared by using yttria- and calcia-stabilized zirconia powders. Structural and electrical properties were investigated and correlated with chemical composition and preparation conditions. For comparison, additional measurements were carried out on commercial single crystals. The chemical composition was tested by proton-induced X-ray emission (PIXE). The microstructure was investigated by scanning electron microscopy (SEM) and optical microscopy. Structural characterization was obtained by the combined use of X-ray diffraction (XRD) and Raman spectroscopy. This latter technique is a powerful tool for the structural analysis of zirconia because of its capability to distinguish with good sensitivity [12, 13] and a high spatial resolution, i.e. 1 μm [14, 15], between the different polymorphs. Finally, the electrical properties of a set of yttria-stabilized films were studied by means of complex impedance spectroscopy [16].

The present paper deals with the structural and microstructural characterization of plasma-sprayed films, while the electrical properties are discussed in detail elsewhere [16].

2. Experimental detail

2.1. Sample preparation

The samples studied in the present work are plasma-sprayed films, powders used for spraying and commercial single crystals. The preparation of the starting powders from pure chemicals was preferred to the use

0022–2461/88 $03.00 + .12

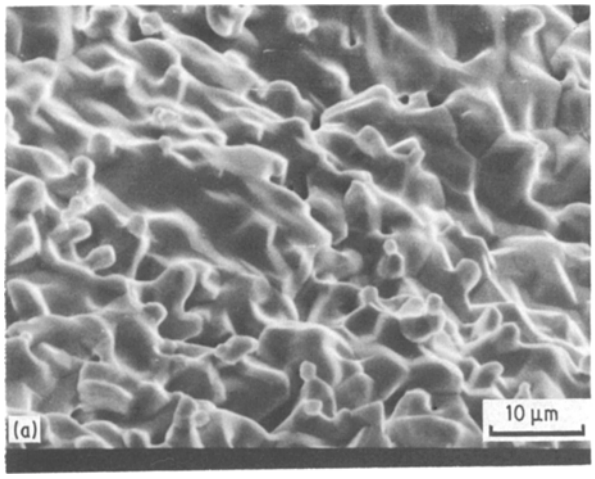

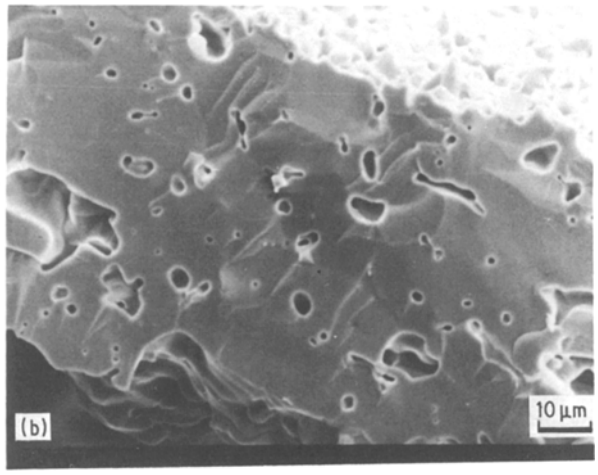

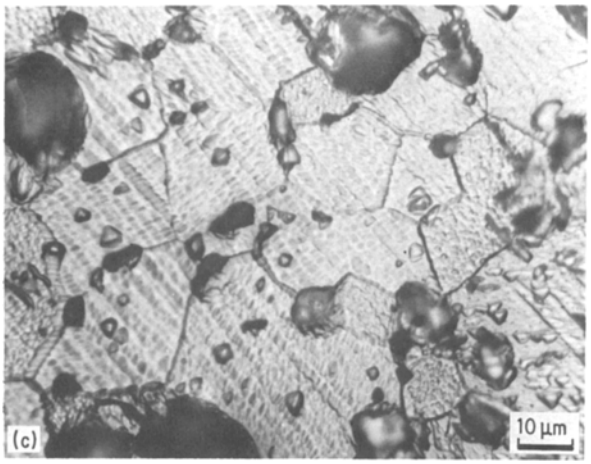

Figure 1 Scanning electron micrographs of (a) the surface and (b) the fractured cross-section of a ZY12-2 film. A micrograph obtained by optical microscope of the polished cross-section of a ZY12-2 sample after etching is shown in (c).

of commercial powders for a better control of the fabrication process parameters.

ZrO_2, Y_2O_3, and CaO (99% pure), supplied by Merck, were mixed in the compositions ZrO_2–8, 10 and 12 mol % Y_2O_3 and ZrO_2–7, 10, 13 and 16 mol % CaO and milled in a tungsten carbide ball mill with tungsten carbide balls. The fine powders were stabilized by heating in air at 1550° C for 24 h. During this process tungsten carbide impurities were oxidized and tungsten oxide (WO_3) evaporated. The powders were calibrated between 37 and 100 μm, the correct grain size for plasma spraying, and coarsened by heating in air at 1550° C for 24 h. Zirconia films were sprayed in air using a Metco plasma spray gun and an argon plasma on flat hot polished steel substrates, coated with a soluble salt. The porous films, 100 to 200 μm thick, were removed from the substrate and densified in vacuum. High temperatures (2000 or 2100° C) were required to improve the density because the material did not contain sintering additives. After 3 h vacuum sintering the films were annealed in air at 1450° C for 3 h to restore the oxygen stoichiometry. Hereafter the samples sintered at 2000 and 2100° C will be labelled 1 and 2, respectively. After the thermal cycling, yttria-stabilized films were free from macroscopic defects, whereas cracks and deformations were observed in calcia-stabilized films.

Zirconia crystals (pure ZrO_2, ZrO_2–4.5, 12, 18 and 24 mol % Y_2O_3), grown by skull melting, were supplied by Ceres (North Billerica, Mass. 01862, USA). Pure zirconia crystals are opaque, multidomain with a monoclinic structure. ZrO_2–4.5 mol % Y_2O_3 crystals are translucent, due to light scattering from a second-phase precipitate structure. In fact they consist of tetragonal and cubic zirconia [13]. Finally samples containing $\geqslant$ 12 mol % of yttria are transparent, crack free, single crystals.

2.2. Characterization techniques

The samples were characterized by using PIXE, XRD Raman spectroscopy, optical microscopy and SEM. The chemical composition was tested by PIXE [17]. The $K\alpha$ and $K\beta$ emissions of zirconium, yttrium and calcium, excited by 2.8 MeV protons, were used to determine the Y(or Ca)/Zr ratio in sprayed films.

An optical microscope and a Jeol scanning electron microscope, equipped with a system for X-ray analysis by EDS, were used for microstructural characterization. In order to measure the average grain size, the cross-section of a few films was polished by means of diamond pastes and etched in an H_2SO_4 : HF (2 : 1) mixture.

XRD measurements were carried out by means of a Philips PW 1130 diffractometer using iron filtered Co$K\alpha$ radiation. The top surfaces of sprayed films were examined, while the powders were spread on to slides for X-ray diffraction.

Raman spectra were obtained by using a double grating Jobin–Yvon HG-2S monochromator. The 488.0 nm line of an Ar^+ laser was chosen to avoid overlapping of Raman spectra and photoluminescence bands.

3. Results

3.1. Stoichiometry

Melting in the plasma arc and vacuum sintering at high temperature can modify film stoichiometry with respect to powder composition. Chemical analysis is therefore necessary for meaningful comparison of the structural and electrical properties of films, sintered pellets and single crystals.

Our sprayed films darkened on vacuum sintering. This effect, due to oxygen loss, is related to the

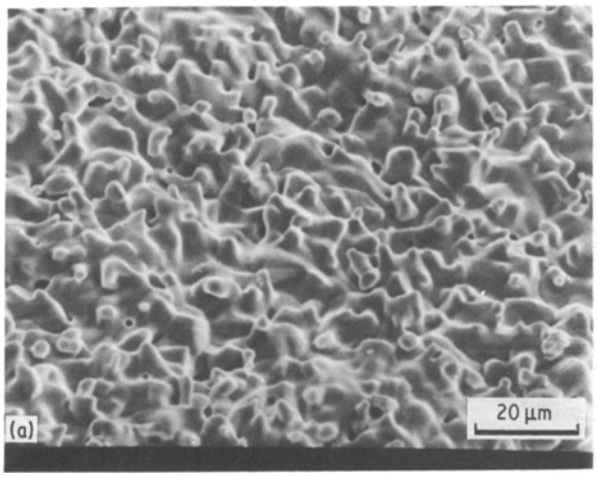

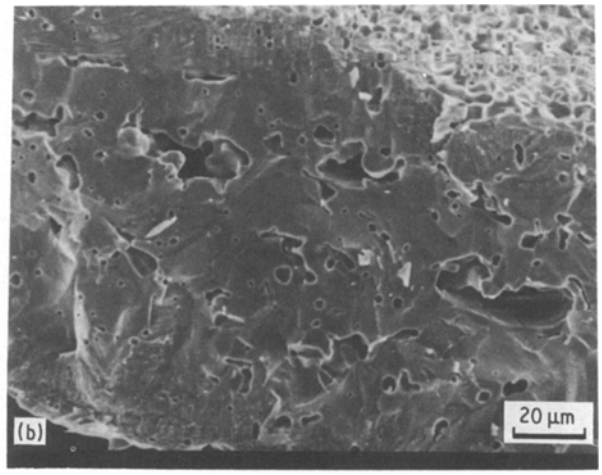

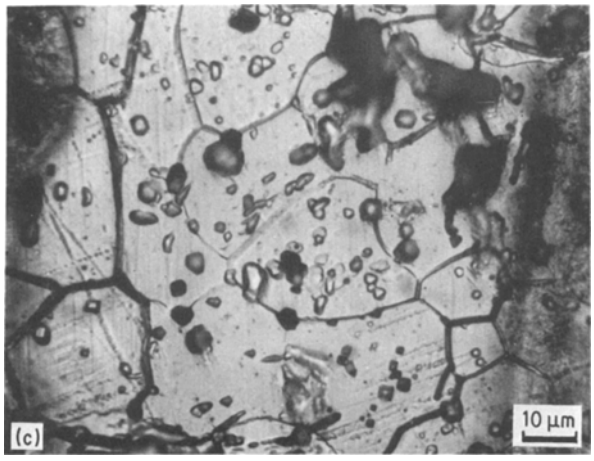

Figure 2 Scanning electron micrographs of (a) the surface and (b) the fractured cross-section of a ZC10-2 film. A micrograph obtained by optical microscope of the polished and etched cross-section of a ZC16-2 is shown in (c).

appearance of a strong, broad, absorption band in the visible region around 0.5 μm [18]. Air annealing at 1450° C for 3 h, however, restored the correct oxygen stoichiometry and changed the dark zirconia films into white, strongly diffusive films.

The cation content was tested by PIXE. Owing to X-ray absorption, only a surface layer, about 4 μm thick, can be investigated in this experiment. The results are reported in Table I. Strong calcium loss occurred in calcia-stabilized zirconia films. Only slight deviations from the nominal composition were observed in yttria-stabilized films, except in the ZY8-2 sample whose actual composition is ZrO_2–14.5 mol % Y_2O_3.

TABLE I Comparison between nominal and experimental M/Zr ratios (M = Y or Ca) measured by PIXE on stabilized zirconia films sintered in vacuum for 3 h at different temperatures

Sample	Stabilizer	T_{sint} (° C)	$(M/Zr)_{nom}$	$(M/Zr)_{exp}$
ZC7-1	CaO(7%)	2000	0.07	0.06
ZC7-2	CaO(7%)	2100	0.07	0.007
ZC10-2	CaO(10%)	2100	0.11	0.004
ZC13-1	CaO(13%)	2000	0.15	0.009
ZC13-2	CaO(13%)	2100	0.15	0.010
ZC16-2	CaO(16%)	2100	0.19	0.002
ZY8-1	Y_2O_3(8%)	2000	0.17	0.21
ZY8-2	Y_2O_3(8%)	2100	0.17	0.34
ZY10-2	Y_2O_3(10%)	2100	0.22	0.24
ZY12-1	Y_2O_3(12%)	2000	0.27	0.25
ZY12-2	Y_2O_3(12%)	2100	0.27	0.25

3.2. Optical and scanning electron microscopy.

3.2.1. ZrO_2–Y_2O_3

Figs 1a and b show scanning electron micrographs of the surface and the fractured cross-section of a ZY12-2 film. The optical micrograph of a polished and etched cross section of the same film is shown in Fig. 1c. Similar results were obtained on the other films. They appear quite dense, with few large voids (10 to 20 μm) which give rise to open porosities only in the thinnest films (< 100 μm). All films are characterized by a well-defined microstructure with an average grain size of about 20 μm (Fig. 1c).

3.2.2. ZrO_2–CaO

Figs 2a and b show the scanning electron micrographs of the surface and the fractured cross-section of a ZC10-2 film. An optical micrograph of the polished and etched cross-section of a ZC16-2 film is shown in Fig. 2c. A well-defined microstructure is exhibited by calcia-stabilized films with an average grain size of about 20 μm. Composition dishomogeneities were detected by EDS analysis. Ca$K\alpha$ maps showed a very low calcium amount near the surface, the nominal content is reached 20 to 30 μm away from the surface.

3.3. X-ray diffraction

X-ray diffractograms were recorded on powders, films and single crystals. In particular the (1 1 1) and (4 0 0) regions were investigated. The reflections from (1 1 1) planes were used to evaluate the molar fraction of monoclinic zirconia [19] while the cubic lattice parameter, a_0, was measured from (4 0 0) reflections. The tetragonal and the cubic phase can be hardly distinguished by XRD. They were identified in our samples by means of Raman measurements, as discussed in the next section.

3.3.1. ZrO_2–Y_2O_3

Figs 3 and 4 show typical XRD patterns of powders and sprayed films in the (1 1 1) and (4 0 0) regions; the

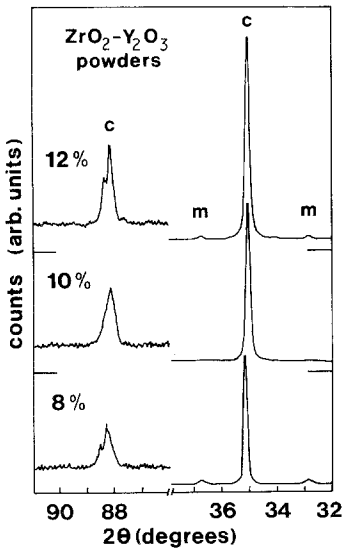

Figure 3 X-ray diffractograms of yttria-stabilized zirconia powders used for spraying (m, monoclinic; c, cubic). The yttria content is indicated in mol %.

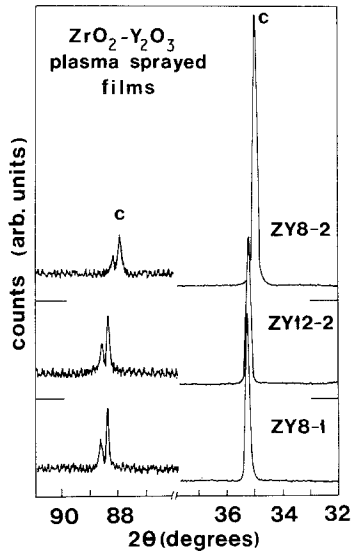

Figure 4 X-ray diffractograms of some yttria-stabilized zirconia films (c, cubic).

cubic lattice parameters of films and single crystals are reported in Table II.

The powders are almost completely stabilized in the cubic phase (Fig. 3). The reflection from the (4 0 0) plane of the cubic phase is observed around $2\theta = 88.2°$. The doublet, due to the $K\alpha_1$ and $K\alpha_2$ components of the cobalt line, is not well resolved (Fig. 3), particularly in the ZrO_2–10 mol % Y_2O_3 sample, indicating that the powders are not well crystallized. As expected, the doublet shifts towards lower angles, i.e. the lattice spacing, d, increases, as yttria content increases.

A few per cents of monoclinic zirconia were detected in powders with 8 and 12 mol % yttria. In the XRD pattern of the latter, an additional very weak peak at $2\theta = 34°$, due to pure Y_2O_3, was observed. In the powder with 10 mol % yttria the monoclinic (1 1 1) and (1 1 $\bar{1}$) peaks can be hardly detected (Fig. 3), traces of monoclinic zirconia were found only by using Raman scattering (see Section 3.4).

Plasma-sprayed film diffractograms show sharp reflections from the (1 1 1) and (4 0 0) planes of the cubic phase (Fig. 4) and in particular the (4 0 0) doublet is well resolved. The cubic lattice parameter, a_0, of most of the sprayed films ranges between 0.5132 and 0.5136 nm (Table II). The expected trend, i.e. the increase of the lattice parameter with the actual yttria content, is well verified. In particular the anomalously high value of a_0 (0.5150 nm) measured on the ZY8-2 film, prepared with ZrO_2–8 mol % Y_2O_3 powders, is consistent with the composition evaluated from PIXE data (ZrO_2–14.5 mol % Y_2O_3).

TABLE II Cubic lattice parameters measured on plasma-sprayed films and crystals of yttria-stabilized zirconia

Sample	Y_2O_3 (mol %)	Lattice param. (nm)
Films ZY8-1	9.5	0.5132
ZY10-2	10.7	0.5134
ZY12-1, 2	11.1	0.5135
ZY8-2	14.5	0.5150
Crystals	4.5	0.5123
	12	0.5150
	18	0.5164
	24	0.5177

3.3.2. ZrO_2–CaO

XRD analysis on CaO-stabilized films were carried out after each step of the preparation process. On increasing the calcia content, a decreasing amount of monoclinic phase is measured in the powders after coarsening, and the 16 mol % CaO powder appears fully stabilized (Fig. 5 and Table III). The cubic (4 0 0) reflection around 88.6° is observed in all the samples, but it is well resolved only in the powders with 13 and 16 mol % CaO.

On the film top surface the monoclinic zirconia content slightly increases on spraying. After high-temperature vacuum sintering, films appear essentially monoclinic (Table III) and only weak reflections from the (1 1 1) plane of tetragonal (or cubic) zirconia are observed. Powders obtained by grinding the sintered films exhibit a lower monoclinic phase content (Table III), showing that the bulk of the film is still stabilized, in agreement with the SEM-EDS results (Section 3.2).

3.4. Raman scattering

Typical Raman spectra of zirconia polymorphs are reported in Fig. 6. They were recorded on pure ZrO_2 (monoclinic), ZrO_2–4.5 mol % Y_2O_3 (tetragonal + cubic) and ZrO_2–12 mol % Y_2O_3 (cubic) crystals.

Eighteen allowed Raman bands are expected for monoclinic zirconia which has C_{4h} symmetry and four

TABLE III Monoclinic zirconia molar fractions measured on calcia-stabilized zirconia samples at different steps of the preparation process (powders used for spraying, sprayed films after vacuum sintering and powders obtained by grinding the films)

CaO (mol %)	Powders	Films	Ground films
7	0.46	–	0.71
10	0.30	0.97	0.21
13	0.07	0.47	0.04
16	0.01	0.96	0.34

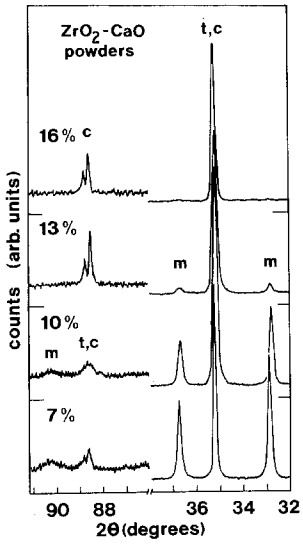

Figure 5 X-ray diffractograms of calcia-stabilized zirconia powders used for spraying (m, monoclinic; t, tetragonal; c, cubic). The calcia content is indicated in mol %.

molecules per unit cell. Sixteen bands are actually observed in the Raman spectrum, which is characterized by intense doublets around 178 to 190, 332 to 346, 474 to 500, 536 to 558 and 614 to 636 cm^{-1}. For tetragonal zirconia, group theory predicts six allowed Raman bands, which are all observed. This spectrum is characterized by strong bands around 260 and 640 cm^{-1} while weaker structures are observed at 147, 320, 464 and 610 cm^{-1}. A broad continuum extending from 0 to 650 cm^{-1} is typical of the cubic zirconia spectrum. The oxygen vacancies in the anionic sublattice of cubic zirconia lead to the relaxation of the $\vec{k} = 0$ selection rule in light scattering and this results in the activation of all the phonon density of states [20]. The polarized components of this spectrum have been recently measured and the phonon density of state calculated by Ishigame and Yoshida [21].

3.4.1. ZrO_2–Y_2O_3

Firstly let us consider the Raman spectra of yttria-stabilized zirconia powders (Fig. 7). All these spectra

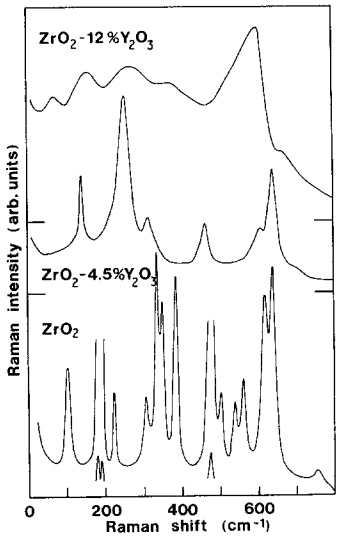

Figure 6 Raman spectra of pure ZrO_2 (monoclinic), ZrO_2–4.5 mol % Y_2O_3 (tetragonal + cubic) and ZrO_2–12 mol % Y_2O_3 (cubic) zirconia crystals.

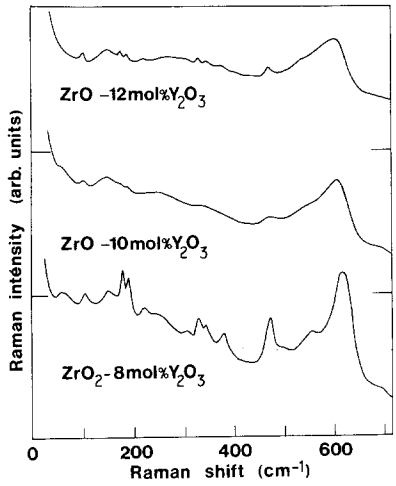

Figure 7 Raman spectra of yttria-stabilized zirconia powders used for spraying.

are characterized by a broad continuum extending from 0 to 650 cm^{-1}, with a rather sharp decrease around 600 cm^{-1}. This feature indicates the presence of cubic zirconia. Weak peaks around 104, 178 to 188 and 474 cm^{-1}, characteristic of the monoclinic phase, can be detected in all the powders. It is pointed out that the ZrO_2–10 mol % Y_2O_3 powder X-ray diffractogram shows only cubic phase peaks (Fig. 3).

Raman spectra of some films, shown in Fig. 8, indicate that only the cubic phase is present after spraying and sintering. Few differences in the band shape, however, are observed in these spectra, depending on the sample composition. The ZY12-2 and the ZY8-1 spectra are characterized by an intense band around 610 to 620 cm^{-1} and by weaker structures around 60, 150 and 480 cm^{-1}. On the other hand, the ZY8-2 film shows a broader spectrum with the main band of the cubic phase shifted downwards to 600 cm^{-1}. Different heat treatments, i.e. sintering at 2000 or 2100° C, do not affect the Raman spectra. In effect the spectra of ZY12-1 and ZY12-2 films, which have the same composition (11.1 mol % Y_2O_3), are identical.

3.4.2. ZrO_2–CaO

Raman spectra of calcia-stabilized zirconia powders are reported in Fig. 9. They are in satisfactory agreement with the phase diagrams of the ZrO_2–CaO

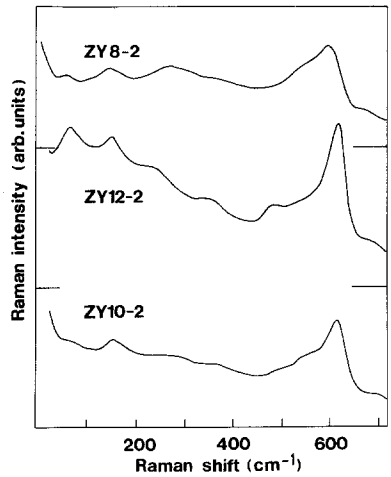

Figure 8 Raman spectra of yttria-stabilized zirconia-sprayed films.

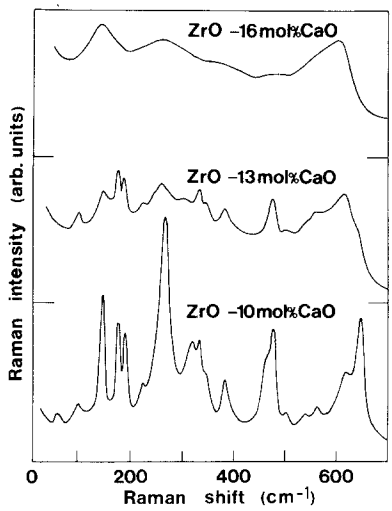

Figure 9 Raman spectra of calcia-stabilized zirconia powders used for spraying.

system reported in the literature [22]. In fact the cubic phase content increases with calcium oxide, as shown by the growth of the broad background between 0 and 650 cm^{-1}, while the tetragonal and monoclinic phases are present only in powders with 7, 10 and 13 mol % CaO.

Raman scattering revealed an anomalously high content of monoclinic and tetragonal zirconia in films after vacuum sintering. Moreover the Raman peak intensities were dependent on the laser beam position in the sample indicating phase distribution variations [23].

All the investigated zirconia samples showed intense luminescence bands. Two groups of bands, around 18 100 and 19 100 cm^{-1}, respectively, were assigned to erbium traces [23, 24]. The intensity, frequency and shape of these bands are related to the structure of the host matrices [24]. In the calcium-stabilized zirconia samples (powders and sintered pellets) an additional strong band was observed around 14 000 cm^{-1}. The disappearance of this band in the sprayed films, exhibiting a strong calcium loss at the surface, suggests that it is in some way related to the calcium content. It could be due to electrons trapped in oxygen vacancies bonded to calcium ions. The interpretation of these complex luminescence spectra, however, requires further investigation.

4. Discussion

Firstly the yttria–zirconia system will be considered. Plasma-sprayed films, after high-temperature vacuum sintering and air annealing, are dense, with few large voids and no open porosity. XRD and Raman measurements show that the films are fully stabilized in the cubic phase, while complex impedance measurements [16] give bulk conductivities and activation energies similar to those of single crystals with the same composition.

However, the knowledge of the actual film composition is necessary for a meaningful interpretation of these results. In fact PIXE measurements indicate some discrepancies between the nominal and the actual stoichiometry. Particularly ZY8-1 and ZY8-2 films, prepared with a ZrO_2–8 mol % Y_2O_3 powder, show a significant increase of the Y/Zr ratio on spraying and vacuum sintering. If the actual compositions are considered, the structural and the electrical properties are in agreement with the results reported in the literature for crystals [25, 26] and sintered specimens [27].

In spite of this fact, our plasma-sprayed films display structural properties quite different with respect to previously published data on sprayed coatings [9–11]. Many authors found significant amounts of tetragonal and monoclinic zirconia even in films with 10 or 12 mol % yttria [9–11]. Very likely this discrepancy arises from different initial phase distribution in the powders used for spraying and from the film sintering process.

The results obtained on calcia-stabilized films are still unsatisfactory. Cracks and deformations were observed after high-temperature vacuum sintering. Evidence of a large calcium loss at the surface with an anomalous increase in the monoclinic zirconia content was found by PIXE, SEM-EDS and XRD analysis.

Recently traces of monoclinic zirconia and an irreversible increase in emissivity were observed in sprayed zirconia layers after heat treatments in vacuum (10^{-4} mm Hg) at temperatures higher than 1800 K [28]. In effect our XRD measurements show that the amount of monoclinic zirconia dramatically increases on high-temperature vacuum sintering. This fact is probably related to the segregation and preferential evaporation of calcium oxide during low pressure (about 10^{-4} torr) high-temperature sintering. In fact, around 2000° C calcium oxide has a rather high vapour pressure (about 4×10^{-2} torr [29]) and calcium exhibits a high diffusion coefficient in zirconia (about 8×10^{-11} cm^2 sec^{-1} [30]). The CaO concentration distribution observed along the cross-section of our samples is similar to that reported for MgO-stabilized ZrO_2 [31] annealed in vacuum at 1920° C, and is characteristic of calcium diffusion-controlled evaporation [32]. The transformation of tetragonal zirconia into monoclinic zirconia, which occurs with a 4 to 5% volume change, is probably responsible for the observed cracks and deformations.

In conclusion, plasma-sprayed electrolytes with different compositions in yttria–zirconia and calcia–zirconia systems were prepared and studied. It is shown that yttria-stabilized zirconia films have structural and electrical properties [16] suitable for application as solid electrolytes, whereas in the case of calcia-stabilized films, the preparation conditions have to be modified, and in particular high-temperature vacuum sintering has to be avoided.

In fuel cell stacking fabrication, the sprayed solid electrolyte is deposited on to a mechanically stable substrate, for example a porous alumina tube [4]. The sintering temperature in this case is strongly limited. Further investigations are therefore required to obtain sufficiently dense as-sprayed layers. In particular, plasma-spray deposition under low pressure or in vacuum [33] could improve the as-sprayed film density.

Acknowledgements

We thank P. Redaelli and M. G. Marcazzan (Cise) for PIXE analysis. This work was supported by the Progetto Finalizzato Energetica 2 of CNR-ENEA.

References

1. E. C. SUBBARAO and H. S. MAITI, *Solid State Ionics* **11** (1984) 317.
2. B. C. H. STEELE, in Proceedings of the VI CIMTEC – World Congress on High Tech Ceramics, Milano, 24–28 June, 1986, edited by P. Vincenzini (Elsevier, Amsterdam, 1987) p. 105.
3. A. O. ISENBERG, *Solid State Ionics* **3/4** (1981) 431.
4. Y. OHNO, S. NAGATA and H. SATO, in Proceedings of the 15th Intersociety Energy Conversion Engineering Conference, Seattle, 18–22 August, 1980 (American Institute of Aeronautics and Astronautics, 1980) p. 881.
5. D. C. FEE, P. E. BLACKBURN, D. BUSCH, T. D. CLAAR, D. W. DEES, J. DUSEK, B. FLANDERMEYER, R. FOUSEK, T. E. KRAFT, C. C. MCPHEETERS, F. C. MRAZEK, R. B. POEPPEL, S. A. ZWICK and J. P. ACKERMAN, in Proceedings of the 1985 Fuel Cell Seminar, Tucson, 19–22 May, 1985, p. 111.
6. M. CROSET, J. P. SCHNELL, G. VELASCO and J. SIEJKA, *J. Appl. Phys.* **48** (1977) 775.
7. A. NEGHISHI, K. NOZAKI and T. OZAWA, *Solid State Ionics* **3/4** (1981) 443.
8. M. MIYAYAMA, H. INOUE and H. YANAGIDA, *J. Amer. Ceram. Soc.* **66** (1983) C-164.
9. R. A. MILLER, R. G. GARLICK and J. L. SMIALEK, *Ceram. Bull.* **62** (1983) 1355.
10. R. A. MILLER and C. E. LOWELL, *Thin Solid Films* **95** (1982) 265.
11. N. IWAMOTO, N. UMESAKI and S. ENDO, *ibid.* **127** (1985) 129.
12. A. FEINBERG and C. H. PERRY, *J. Phys. Chem. Solids* **42** (1981) 513.
13. C. H. PERRY, D. W. LIU and R. P. INGEL, *J. Amer. Ceram. Soc.* **68** (1985) C-184.
14. D. R. CLARKE and F. ADAR, *ibid.* **65** (1982) 284.
15. G. KATAGIRI, H. ISHIDA, A. ISHITANI and T. MASAKI, in Proceedings of the 3rd International Conference on Science and Technology of Zirconia, Tokyo, 9–11 September 1986, edited by Sōmiya, Advances in Ceramics, Vol. 24, in press.
16. G. CHIODELLI, A. MAGISTRIS, M. SCAGLIOTTI and F. PARMIGIANI, *J. Mater. Sci.*, **23** (1988) 1159.
17. I. V. MITCHELL and K. M. BARFOOT, *Nucl. Sci. Applic.* **1** (1981) 99.
18. V. I. ALEKSANDROV, S. K. BATYGOV, M. A. VISHNYAKOVA, YU. K. VORON'KO, V. F. KALABUKHOVA, S. V. LAVRISCHCHEV, E. E. LOMONOVA, V. A. MYZINA and V. V. OSIKO, *Sov. Phys. Solid State* **26** (1984) 799.
19. R. A. MILLER, J. L. SMIALEK and R. G. GARLICK, in Proceedings of the 1st International Conference on Science and Technology of Zirconia, Cleveland, 16–18 June, 1980, edited by A. H. Heuer and L. W. Hobbs, Advances in Ceramics, Vol. 3, p. 241.
20. V. G. KERAMIDAS and W. B. WHITE, *J. Phys. Chem. Solids* **34** (1973) 1873.
21. M. ISHIGAME and E. YOSHIDA, *Solid State Ionics* **23** (1987) 211.
22. V. S. STUBICAN and J. R. HELLMANN, in Proceedings of the 1st International Conference on Science and Technology of Zirconia, Cleveland, 16–18 June 1980, edited by A. H. Heuer and L. W. Hobbs, Advances in Ceramics, Vol. 3, p. 25.
23. G. LANZI, P. MILANI, F. PARMIGIANI, D. RICHON, G. SAMOGGIA and M. SCAGLIOTTI, in Proceedings of the VI CIMTEC – World Congress on High Tech Ceramics, Milano 24–28 June 1986, edited by P. Vincenzini (Elsevier, Amsterdam, 1987) p. 1925.
24. G. LANZI, P. MILANI, F. PARMIGIANI, G. SAMOGGIA and M. SCAGLIOTTI, in Proceedings of the 3rd International Conference on Science and Technology of Zirconia, Tokyo, 9–11 September 1986, edited by Sōmiya, Advances in Ceramics, Vol. 24, in press.
25. R. P. INGEL and D. LEWIS III, *J. Amer. Ceram. Soc.* **69** (1986) 325.
26. S. IKEDA, O. SAKURAI, K. UEMATSU, N. MIZUTANI and M. KATO, *J. Mater. Sci.* **20** (1985) 4593.
27. S. BADWAL, *ibid.* **19** (1984) 1767.
28. G. A. ZHOROV and B. M. ZAKHAROV, *Teplofizika Vysokikh Temperatur* **18** (1980) 745.
29. G. V. SAMSONOV, (ed.), "The Oxide Handbook", 2nd Edn. (IFI Plenum, New York, 1983) p. 148.
30. W. H. RHODES and R. E. CARTER, *J. Amer. Ceram. Soc.* **49** (1966) 244.
31. Y. SAKKA, Y. OISHI and K. ANDO, *ibid.* **69** (1986) 111.
32. T. SATA and Y. UCHIDA, *Yogyo Kyokaishi* **79** (1971) 110.
33. H. GRUNER, *Thin Solid Films* **118** (1984) 409.

Received 4 September 1987
and accepted 11 January 1988